Magnetic Ground State of Pure and Doped $CeFe_2$

L. Paolasini,[1] B. Ouladdiaf,[2] N. Bernhoeft,[3] J-P. Sanchez,[3] P. Vulliet,[3] G. H. Lander,[4] and P. Canfield[5]

[1]*European Synchrotron Radiation Facility, Boîte Postale 220, F-38043 Grenoble Cedex, France*
[2]*Institut Laue Langevin, Boîte Postale 156, 38042 Grenoble Cedex, France*
[3]*Département de Recherche Fondamentale sur la Matière Condensée, SPSMS, CEA, 38054 Grenoble Cedex 9, France*
[4]*European Commission, JRC, Institute for Transuranium Elements, Postfach 2340, D-76125 Karlsruhe, Germany*
[5]*Ames Laboratory, Iowa State University, Ames, Iowa 50011*

(Received 26 September 2002; published 4 February 2003)

A combination of neutron elastic and inelastic, resonant x-ray scattering, and ^{57}Fe Mössbauer experiments are used to determine the unusual magnetic ground state of $CeFe_2$. The complementarities between different time-scale techniques may allow one to understand the dynamic features of the ground state in $CeFe_2$ and its pseudobinary compounds, and how the frustration of Fe tetrahedra leads the appearance of antiferromagnetic fluctuations in the presence of ferrimagnetism. The resulting model can be used to rationalize many of the unusual and conflicting experimental results reported for this material in the literature.

DOI: 10.1103/PhysRevLett.90.057201 PACS numbers: 75.25.+z, 61.18.Fs, 75.30.Ds

Rare-earth iron phases of composition RFe_2 frequently crystallize in the fcc Laves-phase structure and are simple ferro(ferri)magnets [1]. $CeFe_2$ is a remarkable exception. Early studies, both theoretical and experimental, suggested that due to the strong hybridization of the Ce valence band states with the Fe $3d$ electrons [2], the ground state might be more complicated. This was illustrated by reports of antiferromagnetism seen in the neutron-diffraction patterns of the pure compound [3] and the fact that doping $CeFe_2$ with a small amount of many different materials produced an antiferromagnetic (AF) ground state [4,5]. The production of large single crystals of $CeFe_2$ opened the experimental avenue to the magnetic inelastic response function [6]. In addition to the ferromagnetic spin waves, surprisingly strong AF fluctuations were found around the lattice point $(\frac{1}{2}, \frac{1}{2}, \frac{1}{2})$ at the Brillouin zone (BZ) boundary [7].

In this Letter we clarify the ground state of $CeFe_2$ by examining, with neutron elastic and inelastic scattering, resonant x-ray magnetic scattering (RXMS) and the ^{57}Fe Mössbauer effect, single crystals of 7% Co doped $CeFe_2$ ($a_0 = 7.296$ Å), grown via a solution of excess cerium as described in Ref. [8]. This material becomes ferrimagnetic (F) below 210 K, but the doping stabilizes an AF ground state so that a discontinuous transition occurs at $T_N = 69$ K with an ordered wave vector of $Q_0 = \langle \frac{1}{2}, \frac{1}{2}, \frac{1}{2} \rangle$. These values are in agreement with those in the literature [5] and confirm the doping concentration as $7\% \pm 1\%$.

To illustrate the nature of the problem, and the connection between pure and doped $CeFe_2$ materials, we show in Fig. 1 the spin-wave dispersion curves of doped $CeFe_2$ in the F phase (upper panel) and AF phase (lower panel) [9]. The upper panel shows the in-phase precession mode of iron spin waves [7] propagating from the BZ centers (fit with the continuous lines), and the linear AF (broken lines) spin-wave dispersion from the AF point $(\frac{3}{2}, \frac{3}{2}, \frac{3}{2})$, which is a crystallographic BZ boundary. Surprisingly, these coexist in this nominal F state. This situation is similar to that found in pure $CeFe_2$ except for the magnitude of the AF spin-wave gap [6]. In $CeFe_2$ the AF gap falls to ~ 1 meV as the temperature is lowered to 5 K. This small gap may explain how measurable intensity is seen at the AF position when diffractometers (which have no energy discrimination) are used to examine $CeFe_2$ [3]. In fact, the AF state remains *dynamic* in $CeFe_2$, but is stabilized with doping or pressure [10]. In the lower panel of Fig. 1, which is in the truly AF state of the doped material, the ferromagnetic spin waves have disappeared, the AF gap is increased, and the unit cell is rhombohedral (angle 90.31°). The transition at T_N is discontinuous with a volume contraction of 0.18%. The absence of any measurable distortion in the F state is odd in $CeFe_2$, especially when all the other RFe_2 materials (except $GdFe_2$) distort, and this is a point to which we shall return. It is worth noting here that the AF state is unstable against quite small magnetic fields, which induce a F state [7]. This transition has been the subject of considerable work as large magnetoresistance effects of up to 60% are observed [5], but we shall not address this issue here.

The next technique of interest is RXMS, an element selective technique where the incident photon energy is tuned to an absorption edge [11,12]. In these experiments (ID20 at the European Synchrotron Radiation Facility, Grenoble) a σ-polarized photon beam is incident on the crystal (111) face and the intensity of the scattered radiation may be monitored as a function of incident photon energy, temperature, the scattered polarization state (either σ or π), and the azimuthal angle of rotation ψ about the scattering vector [13]. In these experiments the rhombohedral splitting related to the crystallographic distortion is sufficiently large so that we were able, with a beam

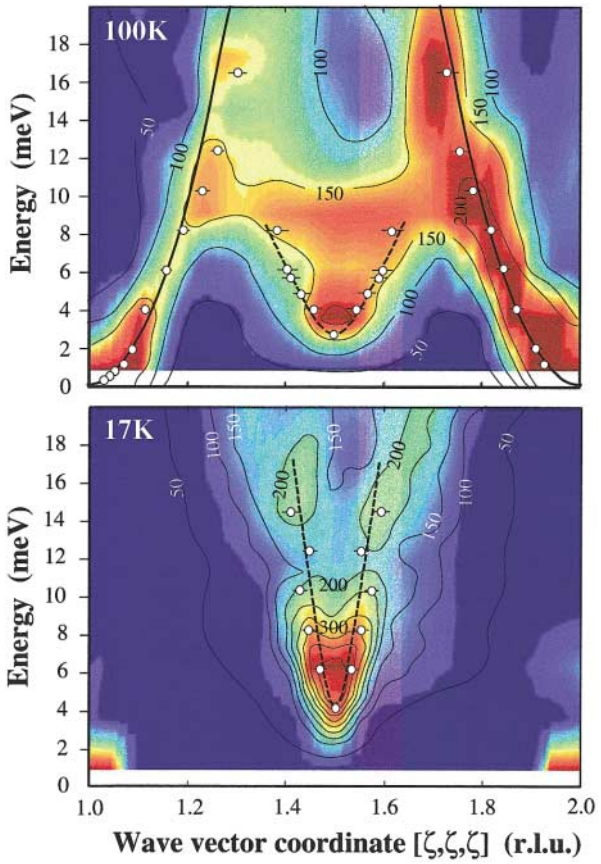

FIG. 1 (color). Contour plots of the dynamical magnetic susceptibility $\chi''(\mathbf{Q}, \omega)$ determined by inelastic neutron scattering at the Laboratoire Léon Brillouin (Saclay, France) around the Brillouin zone boundary $(\frac{3}{2}, \frac{3}{2}, \frac{3}{2})$, and along the [111] direction. The data are collected at 100 K in the F phase (upper panel) and at 17 K in the AF phase (lower panel). $\chi''(\mathbf{Q}, \omega)$ is obtained collating both constant-Q and constant-E scans, after subtraction of background and phonon contributions, and renormalization of the signal by the Bose factor. The data points (open circles) used for the fits are obtained by deconvolution of constant-E scans with the instrument resolution [9]. The thick lines are the fit of the parabolic F (continuous lines) and of the linear AF (broken lines) spin wave dispersions. Measurements in different Brillouin zones establish that all the inelastic response is associated with the Fe spins [6]. The response at 100 K (above T_N as in top frame) shown here for doped compound is identical to that found in pure $CeFe_2$ as discussed in Ref. [6].

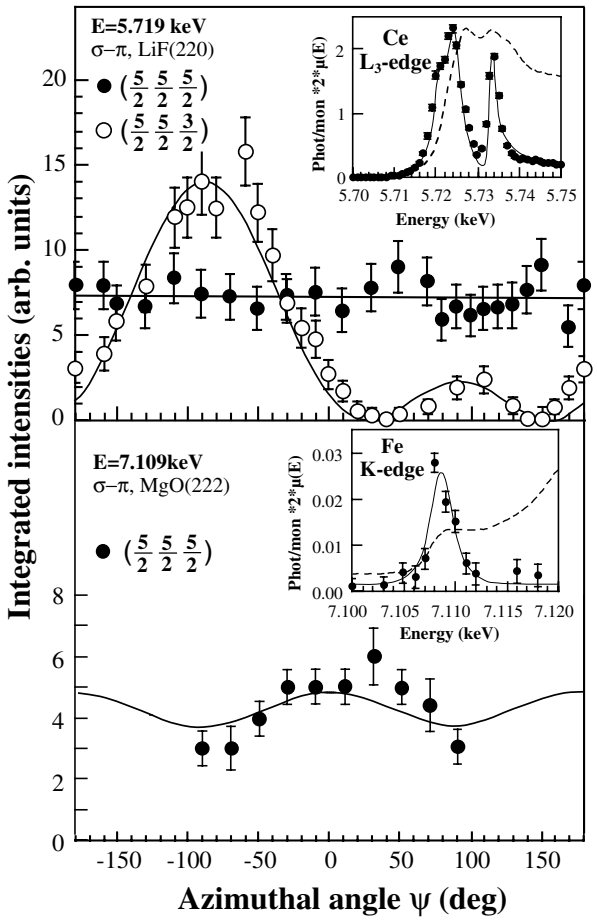

FIG. 2. Azimuthal dependence of resonant magnetic x-ray scattering intensities of the reflections $(\frac{5}{2}, \frac{5}{2}, \frac{5}{2})$ (black points) and $(\frac{5}{2}, \frac{5}{2}, \frac{3}{2})$ (open points) at Ce L_3 edge (upper panel) and Fe K edge (lower panel), taken at 12 K in the σ-π channel. The lines are the calculations of the angular dependence of the resonant intensities with the Ce and the Fe moment directions aligned as shown in Fig. 3. The insets show the energy dependence of the magnetic Bragg reflection $(\frac{5}{2}, \frac{5}{2}, \frac{5}{2})$ at the Ce L_3 edge (upper) and Fe K edge (lower), and the broken lines show the absorption coefficients determined by fluorescence yield at the Ce L_3 edge and the Fe K pre-edge.

size of 0.2×0.2 mm^2, to select a *single* magnetic domain. Moreover, the analysis of the integrated intensities is particularly favorable for a fcc lattice with a magnetic propagation vector $\langle \frac{1}{2}, \frac{1}{2}, \frac{1}{2} \rangle$, because only one magnetic domain contributes to each magnetic Bragg satellite.

The scattered photon intensity as a function of energy is shown in the two insets in Fig. 2. The positions of the peaks with respect to the fluorescence spectrum indicate that both the Ce L_3 pre-edge (5.720 keV) and the Fe K pre-edge (7.109 keV) contain the quadrupole ($E2$) transition. For Ce L_3 this signifies a transition $2p_{3/2} \rightarrow 4f$ and at the Fe K edge a transition $1s \rightarrow 3d$. The observed intensities are sensitive to *moment directions* of the Ce $4f$ and Fe $3d$ states. For the specular reflection $(\frac{5}{2}, \frac{5}{2}, \frac{5}{2})$ no azimuthal dependence is found at the Ce L_3 edge in the σ-π channel, indicating a polarization parallel to the [111] crystallographic direction (solid points in upper panel of Fig. 2). In addition, no signal was found in the σ-σ channel, so that the dominating term in the $E2$ cross section is $F^{(1)}$, as expected, and this makes the calculation of the azimuthal dependence of the intensity straightforward [12]. A verification of the direction of the Ce $4f$ moments may be made by examining the off-specular reflection $(\frac{5}{2}, \frac{5}{2}, \frac{3}{2})$, as shown by the open points in the upper panel. In this case the scattering vector makes an angle $\alpha = 58.25°$ with the Ce magnetic moment direction (assumed parallel

to the local $[11\bar{1}]$ direction), and so with changing the azimuthal angle ψ there is a precession of this moment. The line through the points is a simple geometrical calculation for the scattered intensity assuming the Ce $4f$ moments are parallel to the $[11\bar{1}]$ direction. Clearly the fit is excellent, leaving little ambiguity to the directions of the Ce $4f$ moments.

The results at the Fe K edge, which refer to the Fe $3d$ moments, are more difficult to understand at this stage. Although weaker than the signal at the Ce L_3 edge, the azimuthal dependence of the $(\frac{5}{2}, \frac{5}{2}, \frac{5}{2})$ reflection is not independent of ψ. We shall return to this point.

The small Ce moments of $\sim 0.2\mu_B$ as measured by polarized neutron scattering [14] are thought to be induced by the molecular field of the surrounding Fe sublattice. We now arrive at an apparent contradiction: the presence of neutron-diffraction intensities ([3], and observed in the elastic channel of the experiments reported in Fig. 1) along the $\langle 111 \rangle$ vectors, e.g., $(\frac{h}{2}, \frac{h}{2}, \frac{h}{2})$, proves unambiguously that not all the Fe moments can lie along the [111] direction. Furthermore, the Fe Mössbauer spectrum of doped $CeFe_2$ *cannot* be interpreted in terms of a collinear arrangement of Fe atoms along [111].

In an effort to resolve this apparent paradox we carefully measured the integrated intensities in the neutron-diffraction pattern from a single crystal of the same doped $CeFe_2$ material in the AF state. The elastic neutron-diffraction experiment was performed using the 4-circle spectrometer D10 at the Institut Laue Langevin, Grenoble (France). A set of 330 AF magnetic reflections belonging to the four different magnetic domains was indexed at 1.5 K in the AF phase. The magnetic domains were found to be *equipopulated*, and for a given magnetic domain, a set of 72 magnetic reflections was used in the least square refinement. Previously, with powder diffraction patterns at most five reflections could be measured with sufficient accuracy for the refinement [3]. Not surprisingly, this earlier work was not able to refine noncollinear models and suggested that the Fe moments were collinear at an angle $\Phi \sim 20°$ with the $\langle 111 \rangle$ propagation axis within each domain [3]. In the data analysis we have considered two models, A and B, in which all the Fe atom sites are equivalent and collinear (cubic, space group $Fd\bar{3}m$), as supposed previously [3], or inequivalent and noncollinear (rhombohedric, space group $R\bar{3}m$). The results of our refinement are shown in Table I. Note that model B, Fig. 3, has a net molecular field of a given Fe sublattice along $\langle 111 \rangle$, which then defines the direction of the Ce $4f$ moments.

We now return with this model to the Fe K edge data as a function of the azimuthal angle, ψ, in Fig. 2. The solid line is a model for the azimuthal dependence *assuming* the magnetic structure of Fig. 3, i.e., with the $3e$-Fe moments along [111] and the apical $1b$-Fe moment along $[1\bar{1}0]$. Clearly the data are consistent with this model.

TABLE I. Neutron elastic scattering refinement at $\lambda = 2.36$ Å of the atomic magnetic moments μ of $Ce(Co_{0.07}Fe_{0.93})_2$ in the AF state for two models described in the text. The atomic positions (pos.) refer to the fcc unit cell and Φ is the angle between the magnetic moment and the $\langle 111 \rangle$ propagation axis.

		Model A			Model B		
Atom	pos.	Site ($Fd\bar{3}m$)	μ (μ_B)	Φ (deg)	Site ($R\bar{3}m$)	μ (μ_B)	Φ (deg)
Ce	$\frac{1}{8}\frac{1}{8}\frac{1}{8}$	$8a$	0.08(6)	17	$2c$	0.13(11)	180
	$\frac{3}{8}\frac{3}{8}\frac{7}{8}$	$8a$	0.08(6)	197	$2c$	0.13(11)	0
Fe	$00\frac{1}{2}$	$16d$	1.49(3)	197	$1b$	1.12(7)	90
	$\frac{1}{4}\frac{1}{4}\frac{1}{2}$	$16d$	1.49(3)	17	$3e$	1.61(2)	0
	$\frac{1}{4}0\frac{3}{4}$	$16d$	1.49(3)	17	$3e$	1.61(2)	0
	$0\frac{1}{4}\frac{3}{4}$	$16d$	1.49(3)	17	$3e$	1.61(2)	0
RF^2			22			8.2	
χ^2			55			15	

Several Mössbauer studies have shown that the number and type of inequivalent iron sites in the RFe_2 compounds depend on the orientation of the direction of magnetization with respect to the local [111] axes [15]. According to Fig. 3, and assuming that the hyperfine field (H_{hf}) is parallel to the ion's moment ($H_{hf} \parallel \mu_{Fe}$), one would

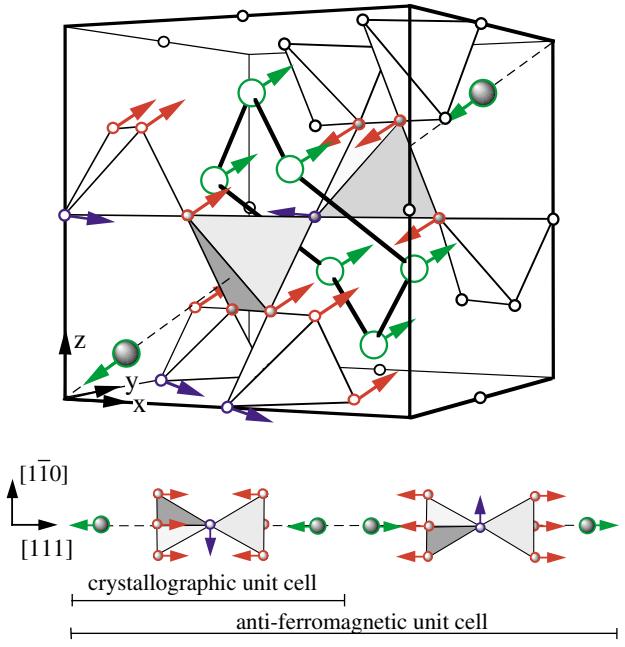

FIG. 3 (color). Magnetic structure in the AF state determined combining neutron and x-ray scattering results (model B in Table I). The Fe sublattice has two inequivalent sites, with $\frac{3}{4}$ of Fe having the magnetic moment direction parallel to [111] (red arrows) and $\frac{1}{4}$ of Fe parallel to the $[1\bar{1}0]$ direction (blue arrows). The Ce magnetic moments point along the [111] direction (green arrows).

expect the occurrence of two inequivalent Fe sites, i.e., a superposition of two sextets of intensity ratio 3:1 with $\theta = 70.5°$ and 90°, respectively, (θ is the angle between the direction of magnetization and the local symmetry axes). This model is however too crude; it cannot reproduce the spectra recorded in the AF state of the Co doped $CeFe_2$ [16] on account of anisotropic dipolar contributions to H_{hf} which play an important role as shown previously [15]. All four Fe ions on the tetrahedra could be inequivalent and the angle θ' between H_{hf} and the local symmetry axes deviate from the nominal θ angles given above. In addition, the rhombohedral distortion and the substitution of Fe by Co lead to further spreads of H_{hf} and θ' [17]. The spectra were thus fitted allowing a distribution of both H_{hf} and θ' while keeping the same value for the quadrupole splitting ($\frac{1}{2}e^2qQ = -0.55$ mm/s). A good fit to the 4.2 K data was obtained with $\langle H_{hf}\rangle = 145$ kOe ($\sigma_H = 15.6$ kOe) and $\langle\theta'\rangle = 76°$ ($\sigma_{\theta'} = 8°$). The $\langle\theta'\rangle$ value and its standard deviation $\sigma_{\theta'}$ are consistent with the model of Fig. 3 ($\langle\theta\rangle = 75.4°$). They rule out collinear magnetic structures with μ_{Fe} along either the main axes of a cube or a $\langle 112\rangle$ direction [3] (for the latter case $\langle\theta\rangle = 58.3°$).

In the AF state the noncollinear nature of the Fe arrangement (Fig. 3) may be seen as a consequence of geometric frustration [18–20] with the cube diagonal distortion axis driven by the orbit-lattice coupling of the $4f$ states, as is found in other RFe_2 materials [1]. On the other hand, the lack of a distortion in the F state is then mystifying in light of both polarized-neutron [14] and dichroism [21] experiments which indicate the presence of an orbital Ce moment. One possibility is that the F state in pure and doped $CeFe_2$ comprises a set of dynamic, microscopic, volumes [22] based on the AF $\langle 111\rangle$ model-B structure introduced above, having planes of ferromagnetic moments ($1.61\mu_B$/Fe) at the $3e$ positions interleaved with antiferromagnetic apical planes at the $1b$ position ($1.12\mu_B$/Fe). Such a model may reconcile both the inhibition of a lattice distortion in the F state, which is then released by macroscopic domain growth on entering the AF phase, and the saturated moment of $\sim 1.2\mu_B$/Fe observed under high magnetic fields ($1.61 \times 3/4 = 1.2\mu_B$/Fe) [23].

Mössbauer experiments, which show the Fe site hyperfine field does not change on passing from the F to the AF state, indicate an invariant local moment averaged over $\sim 10^{-9}$ s giving a lower limit to the dynamics. These manifestations of slow moment dynamics in pure and doped $CeFe_2$ may also shed light upon discrepancies between the results of neutron [14] and dichroism [21] measurements noted previously [24]. Resonant x-ray magnetic dichroism, which senses the polarization on the Ce site on a time scale of $\sim 10^{-15}$ s, yields systematically higher estimates for orbital polarization closer to those given in band structure calculations than neutron scattering.

Hopefully, these experiments and their interpretation will stimulate further experimental and theoretical studies probing the dynamical nature of the magnetic state in such materials.

We thank Flora Yakhou for help during the RXMS experiments at the ID20 beam line and Bernard Hennion for valuable support on the 1T1 TAS spectrometer at Laboratoire Léon Brillouin.

[1] A. E. Clark, in *Ferromagnetic Materials*, edited by E. P. Wohlfarth (North Holland, Amsterdam, 1980), Vol. 1, p. 531.
[2] O. Eriksson *et al.*, Phys. Rev. Lett. **60**, 2523 (1988).
[3] S. J. Kennedy and B. R. Coles, J. Phys. Condens. Matter **2**, 1213 (1990).
[4] D. F. Franceschini and S. F. da Cunha, J. Magn. Magn. Mater. **51**, 280 (1985); S. B. Roy and B. R. Coles, J. Phys. F: Met. Phys. **17**, L215 (1987).
[5] A complete list of references to previous work may be found in H. Fukuda *et al.*, Phys. Rev. B **63**, 054405 (2001).
[6] L. Paolasini *et al.*, Phys. Rev. B **58**, 12 117 (1998).
[7] A summary of our work on single crystals up to 1999 appears in L. Paolasini and G. H. Lander, J. Alloys Compd. **303–304**, 232 (2000).
[8] P. C. Canfield and Z. Fisk, Philos. Mag. B **65**, 1117 (1992).
[9] More data and pertinent experimental details will be published elsewhere.
[10] T. Fujiwara *et al.*, Physica (Amsterdam) **312B–313B**, 336 (2002).
[11] D. Gibbs *et al.*, Phys. Rev. Lett. **61**, 1241 (1988); J. P. Hannon *et al.*, Phys. Rev. Lett. **61**, 1245 (1988).
[12] J. P. Hill and D. F. McMorrow, Acta Crystallogr. Sect. A **52**, 236 (1996).
[13] URL http://www.esrf.fr/exp_facilities/ID20/.
[14] S. J. Kennedy *et al.*, J. Phys. Condens. Matter **5**, 5169 (1993).
[15] G. J. Bowden *et al.*, J. Phys. C. **1**, 1376 (1968).
[16] J. P. Sanchez, P. Vulliet, and M. M. Abd-Elmeguid, Hyperfine Interact. **133**, 5 (2001), where a part of the Mössbauer work is published.
[17] For 7% Co doping about 29% of the iron atoms have one Co atom in the near neighbor configuration if one assumes a statistical distribution.
[18] R. Ballou *et al.*, Phys. Rev. Lett. **76**, 2125 (1996).
[19] M. J. Harris *et al.*, Phys. Rev. Lett. **79**, 2554 (1997).
[20] S.-H. Lee *et al.*, Phys. Rev. Lett. **84**, 3718 (2000).
[21] A. Delobbe *et al.*, Europhys. Lett. **43**, 320 (1998).
[22] N. Bernhoeft, J. Phys. Condens. Matter **13**, R771 (2001); J. Phys. Soc. Jpn., Suppl. A **70**, 7 (2001).
[23] H. Wada *et al.*, J. Phys. Soc. Jpn. **62**, 1337 (1993).
[24] A. P. Murani and P. J. Brown, Europhys. Lett. **48**, 353 (1999); A. Delobbe *et al.*, Europhys. Lett. **48**, 355 (1999).